Contribution No. 8120 from the Arthur Amos Noyes Laboratories, Division of Chemistry and Chemical Engineering, California Institute of Technology, Pasadena, California 91125

Catalytic Pathways for the Electroreduction of O_2 by Iron Tetrakis(4-*N*-methylpyridyl)porphyrin or Iron Tetraphenylporphyrin Adsorbed on Edge Plane Pyrolytic Graphite Electrodes

Chunnian Shi and Fred C. Anson*

Received March 28, 1990

Spontaneous adsorption of iron tetrakis(4-*N*-methylpyridyl)porphyrin on edge plane pyrolytic graphite electrodes (EPG) from aqueous solutions of the soluble porphyrin produces an adsorbed species that catalyzes the electroreduction of O_2 at potentials notably more positive than can be obtained with electrodes on which the porphyrin does not adsorb (e.g., glassy carbon). Adsorption of insoluble iron tetraphenyl porphyrin (FeTPP) on EPG electrodes produces two surface waves for the adsorbed porphyrin, one prominent and one partially hidden by the response from the EPG surface itself. Only the form of the FeTPP responsible for the latter wave participates in the catalytic reduction of O_2. Possible explanations for the observed behavior are offered that allow the apparently disparate catalytic reactivity exhibited by iron and cobalt porphyrins to be understood as examples of a single mechanistic pattern.

Studies of the catalysis of the electroreduction of O_2 by water-soluble iron porphyrin complexes have been extensive,[1-13] especially by Kuwana and co-workers.[1,2,5-9,11] Although the potentials where the reduction of O_2 proceeds are not as positive as those that can be achieved with the corresponding cobalt porphyrins,[14-16] the iron (but not the cobalt) porphyrins are also catalysts for the reduction of H_2O_2 so that they often provide larger catalytic currents. The potentials where the water-soluble tetrakis(4-*N*-methylpyridyl)iron porphyrin (FeTMPyP) catalyzes the electroreduction of O_2 depend on the electrode material employed. With polished glassy carbon electrodes there is little or no adsorption of the FeTMPyP catalyst on the electrode surface and the reduction of O_2 occurs at potentials close to the formal potential for the Fe^{III}/Fe^{II} couple of the FeTMPyP in solution.[11] By contrast, at pyrolytic graphite electrodes there is strong adsorption of the catalyst and the reduction of O_2 is shifted to potentials much more positive than the formal potential of the Fe^{III}/Fe^{II} couple of the dissolved FeTMPyP.[10] A similar large difference between the formal potential of the Fe^{III}/Fe^{II} centers in adsorbed, insoluble iron porphyrins and the potential where they catalyze the reduction of O_2 has been noted in a previous study where it was pointed out that the difference in potentials was too large to be compatible with a reaction mechanism that involves a rapid reaction between O_2 and the reduced form of the catalyst.[10]

In the present study a likely origin of the large difference in potentials where FeTMPyP catalyzes the reduction of O_2 on glassy carbon and graphite electrodes has been identified. A catalytic mechanism is suggested that is very similar to that exhibited by adsorbed cobalt porphyrins and eliminates the need to search for alternative explanations to understand what had been regarded as the disparate behavior of the two types of metalloporphyrins.

Experimental Section

Materials. Iron(III) *meso*-tetraphenylporphyrin chloride (FeTPPCl, Strem Chemical Co.) was purified by recrystallization twice from benzene/alcohol (1:1). Tetrakis(4-N-methylpyridyl)porphyrin (Strem) was metalated according to the published procedure.[17] UV-vis spectra and electrochemical behavior of the resulting product agreed with literature values.[11] All reagents employed were analytical grade and used without further purification. Solutions were prepared from distilled water that was further purified by passage through a purification train (Barnstead Nanopure). Buffer solutions had the following compositions: pH 0, 1 M H_2SO_4, CF_3COOH, or $HClO_4$; pH 1.0, 0.1 M H_2SO_4 or CF_3COOH; pH 1.2, 0.1 M $HClO_4$ + 0.1 M $NaClO_4$; pH 1.45, 0.1 M $NaHSO_4$ + 0.05 M Na_2SO_4; pH 2.25, 0.4 M $CH_2ClCOOH$ + 0.1 M $CH_2ClCOONa$; pH 3.34, 0.1 M CH_3COOH + 0.026 M CH_3COONa; pH 4.50, 0.1 M CH_3COOH + 0.1 M CH_3COONa; pH 6.00, 0.056 M CH_3COOH + 1.0 M CH_3COONa; pH 7.10, 0.04 M NaH_2PO_4 + 0.04 M Na_2HPO_4; pH 8-9.2, 0.02 M $Na_2B_4O_7$ + HCl or NaOH; pH 9.95, 0.066 M $NaHCO_3$ + 0.066 M Na_2CO_3; pH 13.0, 0.1 M NaOH; pH 14.0, 1.0 M NaOH.

Apparatus and Procedures. A conventional two-compartment electrochemical cell was used. All potentials were measured and are quoted with respect to a saturated calomel reference electrode (SCE). The rotating disk electrodes were constructed by using heat-shrinkable tubing to mount a 5 mm glassy carbon rod (Tokai Carbon Co., Tokyo) or a 6 mm edge plane pyrolytic graphite rod (Union Carbide Co., Chicago, IL) on a stainles steel shaft adapted to fit an ASR2 rotator (Pine Instrument Co.). PAR electrochemical instruments, Models 173, 175, and 179, were used to obtain cyclic voltammograms that were recorded with an x-y recorder (Houston Instruments). A BAS-100 electrochemical analyzer was used to obtain the square wave voltammograms. To calculate the Levich limiting currents at the rotating disk electrodes, the following parameters were used: kinematic viscosity of water, 0.01 cm/s; solubility of O_2 in air-saturated solutions, 0.28 mM; diffusion coefficient for dioxygen, 1.7×10^{-5} cm^2 s^{-1}. The edge plane pyrolytic graphite electrodes were polished with No. 600 SiC paper (3M Co., Minneapolis, MN), which produced a smooth but not reflective surface. The glassy carbon electrodes were polished with 0.05-μm alumina to obtain a mirrorlike surface. The iron tetraphenylporphyrin was applied to the electrodes by transferring a measured volume of a standard solution of the porphyrin in 1,2-dichloroethane to the electrode surface and allowing the solvent to evaporate. Iron tetrakis(4-*N*-methylpyridyl)porphyrin was adsorbed on edge plane pyrolytic graphite electrodes by pipetting a known amount of porphyrins from a standard solution in C_2H_5OH/H_2O (1:1) or directly from solutions of the water-soluble porphyrin as described in the text.

Results

Cyclic Voltammetric Behavior of FeTMPyP in the Absence and Presence of O_2. The reversible voltammetry of FeTMPyP in 0.1 M H_2SO_4 at a polished glassy carbon electrode in the absence of O_2 is shown in Figure 1A. Saturation of the solution with air

(1) Kuwana, T.; Fujihara, M.; Sunakawa, K.; Osa, T. *J. Electroanal. Chem. Interfacial Electrochem.* **1978**, *88*, 229.
(2) Bettelheim, A.; Kuwana, T. *Anal. Chem.* **1979**, *51*, 2257.
(3) Kobayashi, N.; Fujihara, M.; Sunakawa, K.; Osa, T. *J. Electroanal. Chem. Interfacial Electrochem.* **1979**, *101*, 269.
(4) Kobayashi, N.; Matsue, T.; Fujihara, M.; Osa, T. *J. Electroanal. Chem. Interfacial Electrochem.* **1979**, *103*, 427.
(5) Kobayashi, N.; Fujihara, M.; Osa, T.; Kuwana, T. *Bull. Chem. Soc. Jpn.* **1980**, *53*, 2195.
(6) Bettelheim, A.; Chan, R. J. H.; Kuwana, T. *J. Electroanal. Chem. Interfacial Electrochem.* **1980**, *110*, 93.
(7) Forshey, P. A. and Kuwana, T. *Inorg. Chem.* **1981**, *20*, 693.
(8) Dimarco, D. M.; Forshey, P. A.; Kuwana, T. Electrochemical and Spectrochemical Studies of Biological Redox Components. In Advances in Chemistry Series, No. 192; Miller, J. S., Ed.; American Chemical Society: Washington, DC, 1982; Chapter 6.
(9) Forshey, P. A.; Kuwana, T.; Kobayashi, N.; Osa, T. Chemically Modified Surfaces in Catalysis and Electrocatalysis. In Advances in Chemistry Series No. 201; Kadish, K. M., Ed.; American Chemical Society: Washington, DC, 1982; Chapter 25.
(10) Shigehara, K.; Anson, F. C. *J. Phys. Chem.* **1982**, *86*, 2776.
(11) Forshey, P. A.; Kuwana, T. *Inorg. Chem.* **1983**, *22*, 699.
(12) Bettelheim, A.; Ozer, D.; Harth, R.; Murray, R. W. *J. Electroanal. Chem. Interfacial Electrochem.* **1989**, *266*, 93.
(13) Ozer, D.; Harth, R.; Mor, U.; Bettelheim, A. *J. Electroanal. Chem. Interfacial Electrochem.* **1989**, *266*, 109.
(14) Chan, R. J. H.; Su, Y. O.; Kuwana, T. *Inorg. Chem.* **1985**, *24*, 3777.
(15) Bettelheim, A.; Chan, R. J. H.; Kuwana, T. *J. Electroanal. Chem. Interfacial Electrochem.* **1979**, *99*, 390.
(16) Chan, R. J. H.; Ueda, C.; Kuwana, T. *J. Am. Chem. Soc.* **1983**, *105*, 3713.
(17) Hambright, P.; Fleischer, E. B. *Inorg. Chem.* **1970**, *9*, 1757.

0020-1669/90/1329-4298$02.50/0

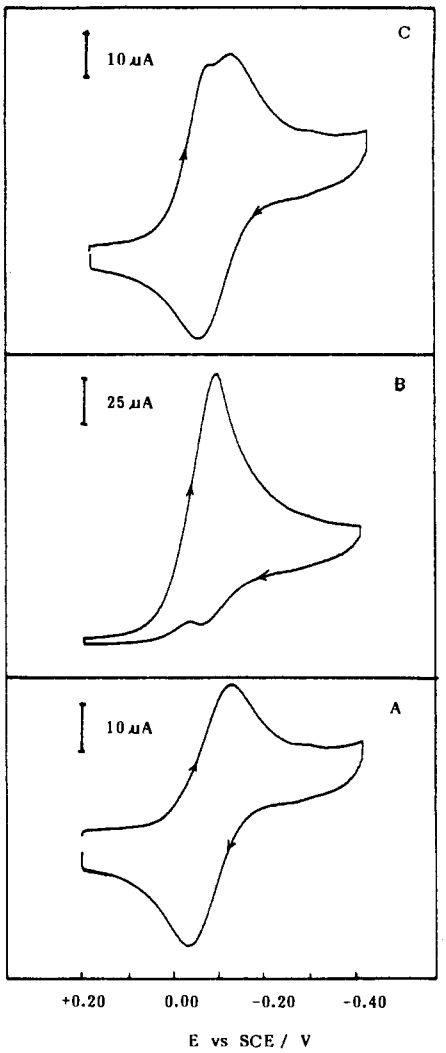

Figure 1. (A) Cyclic voltammetry of 0.99 mM FeTMPyP at a highly polished glassy carbon electrode. (B) Repeat of A after the solution was saturated with air; $[O_2] = 0.28$ mM. (C) Repeat of A in the presence of less O_2; $[O_2] \sim 1.1 \times 10^{-2}$ mM. Supporting electrolyte was 0.1 M H_2SO_4. Scan rate was 50 mV s^{-1}.

causes the reduction current to increase and the anodic wave to diminish as expected for the catalytic reduction of O_2 (Figure 1B). The peak potential of the catalytic wave is very close to cathodic peak of the catalyst itself under the conditions employed in Figure 1B. Increasing the ratio of catalyst to substrate (O_2) causes the O_2 reduction peak to shift to more positive values so that a double peak results (Figure 1C). This is the behavior expected for a system in which both catalyst and substrate are dissolved in solution.[18] Except for the double peaks obtainable at high ratios of catalyst to substrate, the behavior agrees with that reported previously by Forshey and Kuwana.[11]

Quite different behavior results when an edge plane pyrolytic graphic electrode (EPG) is employed to record the voltammograms for FeTMPyP (Figure 2A). Two sets of voltammetric peaks are present labeled I and II in Figure 2A. The formal potential for peak I is close to that of the single peak obtained at glassy carbon electrodes and the peak current increases with the square root of the potential scan rate (Figure 2B) so that it is assignable to the dissolved FeTMPyP complex. The second cathodic peak with a potential near 0.16 V and a peak current that increases linearly with the scan rate (Figure 2C) arises from the adsorbed reactant. It persists for a few scans if the electrode is transferred to pure supporting electrolyte composed of 0.1 M H_2SO_4 and for longer periods in perchlorate supporting electrolytes in which the

(18) Andrieux, C. P.; Blogman, C.; Dumas-Bouchiat, J.-M.; M'Halla, F.; Saveant, J.-M. *J. Electroanal. Chem. Interfacial Electrochem.* **1980**, *113*, 19.

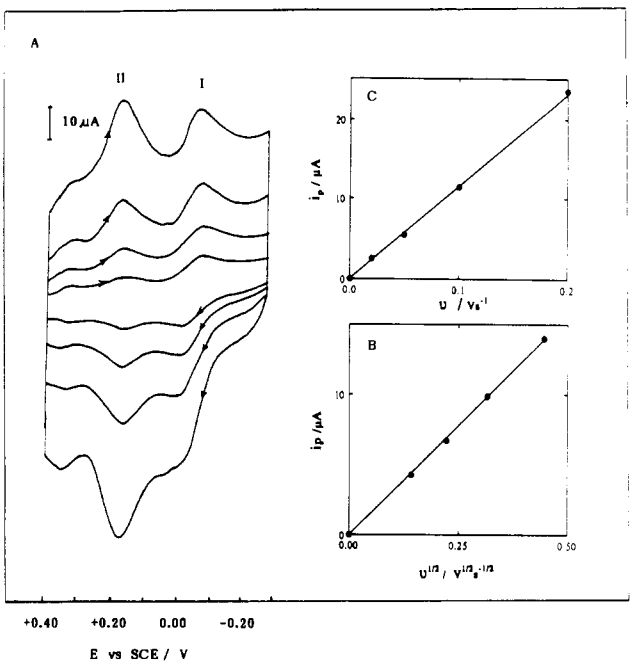

Figure 2. (A) Cyclic voltammetry of 0.3 mM FeTMPyP at an EPG electrode (polished as described in the Experimental Section): supporting electrolye, 0.1 M H_2SO_4; scan rate, 20, 50, 100, 200 mV s^{-1}. (B) Peak currents for peak I in A vs (scan rate)$^{1/2}$. (C) Peak currents for peak II in A vs scan rate.

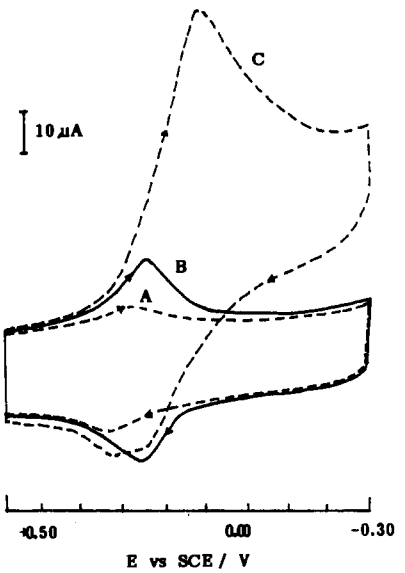

Figure 3. Cyclic voltammetry of FeTMPyP adsorbed on an EPG electrode: (A) background current at the bare EPG electrode; (B) after 4.7 $\times 10^{-10}$ mol cm^{-2} of FeTMPyP was adsorbed on the electrode; (C) repeat of B in an air-saturated solution. Conditions were as follows: supporting electrolyte, 0.1 M $HClO_4$–0.1 M $NaClO_4$; scan rate, 50 mV s^{-1}.

FeTMPyP cation is much less soluble. In Figure 3, curve B is the response obtained when an EPG electrode coated with FeTMPyP is used to record voltammograms in a 0.1 M $HClO_4$–0.1 M $NaClO_4$ supporting electrolyte in the absence of O_2. The adsorbed FeTMPyP gives rise to the symmetrical peak which is centered at 0.25 V in this electrolyte. In the presence of O_2 a catalytic reduction peak appears (curve C in Figure 3) at potentials notably more positive than can be obtained at glassy carbon electrodes in sulfuric acid solutions containing the soluble FeTMPyP (Figure 1B).

Voltammetry at a Rotating Disk Electrode. A current–potential curve recorded at relatively high sensitivity for a rotating EPG disk electrode in a solution of FeTMPyP is shown in Figure 4A. The small wave near 0.35 V is associated with the graphite surface and is present in the absence of the porphyrins. The peak near 0.15 V is independent of the electrode rotation rate and corre-

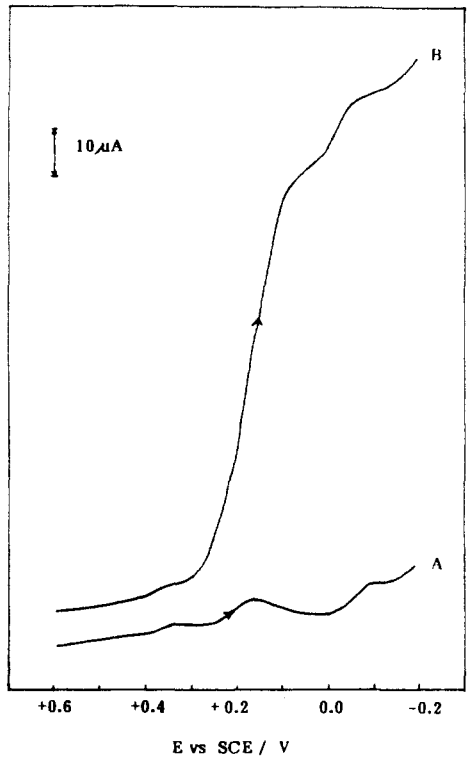

Figure 4. (A) Current–potential curves for 0.2 mM FeTMPyP at a rotating EPG disk electrode in 0.1 M H_2SO_4; electrode rotation rate, 100 rpm. (B) Repeat of A after saturation of the solution with air. The potential was scanned at 20 mV s^{-1}.

sponds to the reduction of the adsorbed FeTMPyP. The reduction of the soluble reactant gives rise to the wave with $E_{1/2}$ near −0.05 V. With an air-saturated solution, the current–potential response shown in Figure 4B is obtained. The catalytic reduction of O_2 proceeds at potentials in the vicinity of the peak for the adsorbed catalyst in curve A and the current on the plateau corresponds closely to that expected for the four-electron reduction of O_2 to H_2O. The magnitude of the second wave, corresponding to the reduction of the dissolved $Fe^{III}TMPyP$, remains essentially unchanged in the presence of O_2 (Figure 4). This behavior shows clearly that the only role played by the dissolved porphyrin in the catalyzed reductions is to supply the $Fe^{III}TMPyP$ that is adsorbed on the electrode surface where it is apparently able to turnover at a rate sufficient to consume all of the O_2 that reaches the electrode. This surmise is confirmed by the Levich[19] and Koutecky–Levich plots[20] shown in Figure 5. Only at the highest rotation rates do the plateau currents for the catalyzed reduction of O_2 begin to deviate from linearity (Figure 5A) and the deviations are too small to produce a measurable intercept in the Koutecky–Levich plot (Figure 5B) which has a slope matching that calculated for the convection-diffusion-limited four-electron reduction of O_2 using the parameters specified in the Experimental Section. Thus, FeTMPyP adsorbed on EPG electrodes is so reactive toward the electroreduction of O_2 that the dissolved catalyst, which is also highly reactive as judged from the behavior observed at glassy carbon electrodes (Figure 1), is merely a spectator to the catalysis obtained at EPG electrodes.

One might expect the catalytic behavior observed with EPG electrodes to become more similar to that at glassy carbon electrodes if a more strongly adsorbed molecule were placed on the surface of the EPG electrode so that the adsorption of FeTMPyP molecules from solution were eliminated or greatly decreased. The disilver derivative of the cofacial dimeric porphyrin examined in a previous study,[21,22] Ag_2FTF4, is very strongly adsorbed on

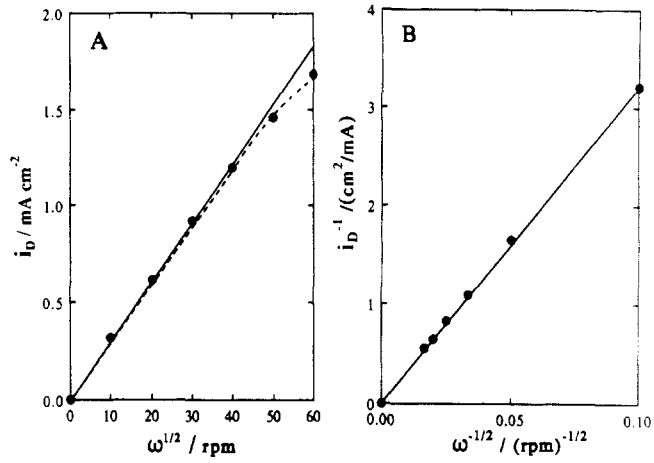

Figure 5. (A) Levich plot of plateau current vs (rotation rate)$^{1/2}$ from curves such as those in Figure 4B. (B) Koutecky–Levich plot of the data from A. The points are the experimental values. The solid lines were calculated for the convection-diffusion-limited four-electron reduction of O_2.

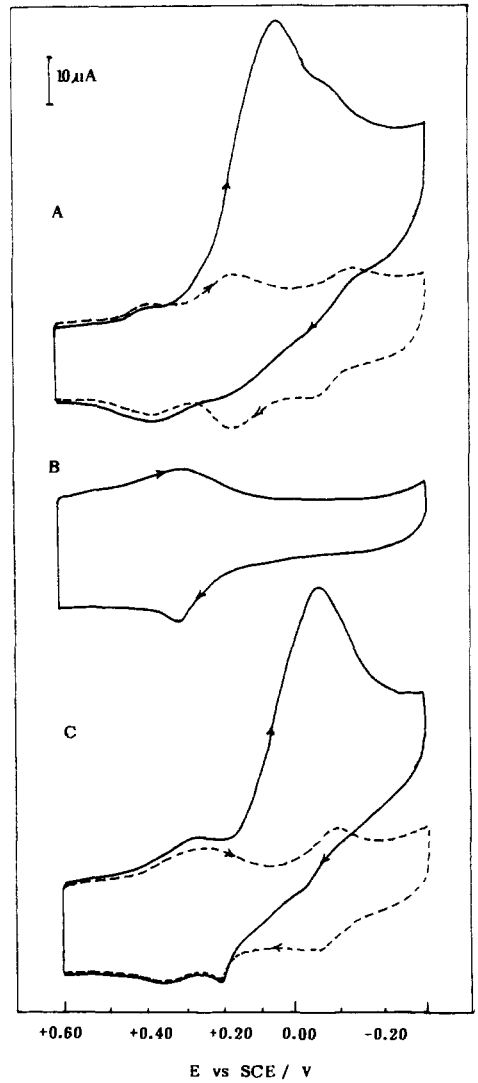

Figure 6. Effect of a strongly adsorbed but catalytically inactive molecule, Ag_2FTF4, on the reduction of O_2 in solutions of FeTMPyP: (A) cyclic voltammetry for 0.2 mM FeTMPyP in the absence of O_2 (dashed line) and in an air-saturated solution (solid line); (B) cyclic voltammogram of an EPG electrode coated with ~10^{-9} mol cm^{-2} of Ag_2FTF4; (C) repeat of A using the electrode from B. Supporting electrolyte was 0.1 M H_2SO_4. Scan rate was 50 mV s^{-1}.

graphite but has no catalytic activity toward the reduction of O_2.[21] Voltammograms recorded in solutions of FeTMPyP and O_2 are

(19) Levich, V. G. *Physicochemical Hydrodynamics*; Prentice-Hall: Englewood Cliffs, NJ, 1962.
(20) Koutecky, J.; Levich, V. G. *Zh. Fiz. Khim.* **1956**, *32*, 1565.
(21) Collman, J. P.; Bencosme, C. S.; Durand, R. R., Jr.; Kreh, R. P.; Anson, F. C. *J. Am. Chem. Soc.* **1983**, *105*, 2699.

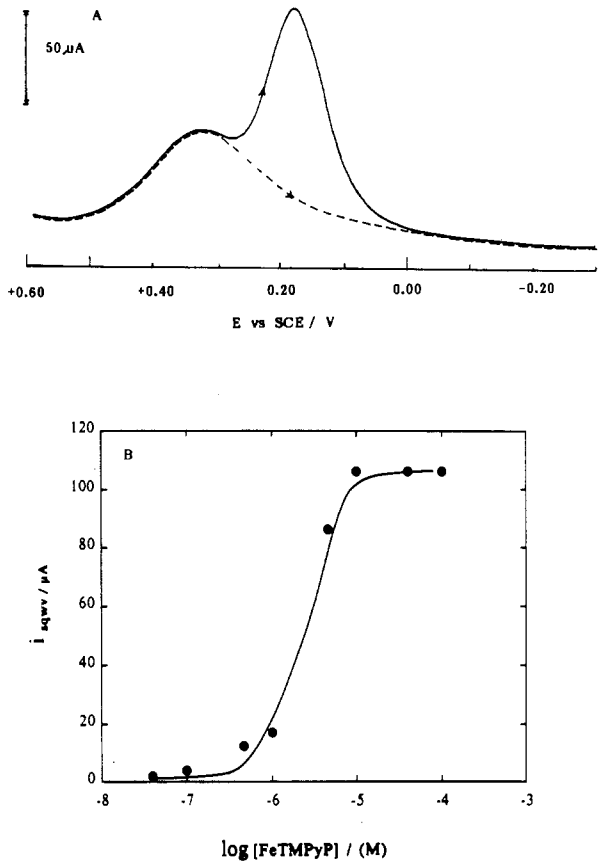

Figure 7. (A) Square wave voltammetry at an EPG electrode: dashed line, background response in the absence of the iron porphyrin; solid line, after addition of 5×10^{-6} M FeTMPyP. (B) Square-wave peak currents for adsorbed FeTMPyP vs its concentration in solution. Supporting electrolyte was 0.1 M H_2SO_4. Square wave parameters were as follows: amplitude, 25 mV; increments, 2 mV per step; frequency, 10 Hz.

shown in Figure 6 before and after the EPG electrode had ca. 10^{-9} mol cm^{-2} of the disilver of cofacial porphyrin applied to its surface. In the presence of the strongly adsorbed Ag_2FTF4 the catalytic wave for O_2 reduction is shifted to near the same potential as is found at glassy carbon electrodes showing that in the absence of catalyst adsorption glassy carbon and EPG electrodes behave similarly, as anticipated.

The quantities of FeTMPyP adsorbed on EPG electrodes from solutions of this porphyrin in 0.1 M H_2SO_4 can be estimated from the areas under voltammetric peaks such as those in Figure 2A. The extent of adsorption becomes independent of the bulk concentration of the porphyrin above ca. 10^{-5} M and reaches ca. 10^{-10} mol cm^{-2}, which corresponds to one monolayer of the porphyrin. Square wave voltammetry[23,24] provides particularly well-formed peaks for adsorbed FeTMPyP as shown in Figure 7A. The square-wave peak for the adsorbed FeTMPyP is readily discerned even when its bulk concentration is too low to produce a detectable square wave response near −0.1 V. A plot of the magnitude of the square-wave peak heights as a function of the concentration of FeTMPyP is shown in Figure 7B. It has the shape expected for an adsorption isotherm and indicates that the adsorption decreases to less than 10% of a monolayer at concentrations below ca. 10^{-6} M.

The effect of decreasing the quantity of adsorbed catalyst on the catalytic wave for the reduction of O_2 is shown in Figure 8. At concentrations so low (e.g., 4×10^{-8} M) that there is essentially no adsorption of the FeTMPyP on the electrode (Figure 7B), the reduction of O_2 is catalyzed only by the dissolved catalyst so that

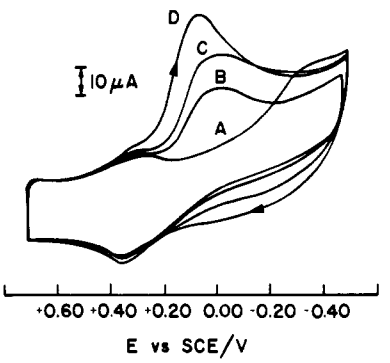

Figure 8. Cyclic voltammograms for the reduction of O_2 at an EPG from air-saturated solutions of FeTMPyP as a function of the concentration of FeTMPyP: (A) 4×10^{-8} M; (B) 4×10^{-7} M; (C) 4×10^{-6} M; (D) 4×10^{-5} M. Supporting electrolyte was 0.1 M H_2SO_4. Scan rate was 50 mV s^{-1}.

the reduction occurs at potentials near −0.2 V (Figure 8A). As the catalyst concentration is increased, more of the catalyst is adsorbed and the reduction of O_2 proceeds more rapidly and at increasingly positive potentials (Figure 8B–D).

The combination of the results we have presented for the catalysis of the reduction of O_2 by the water-soluble FeTMPyP catalyst makes it evident that adsorption is crucial in controlling the potential where the electroreduction of O_2 proceeds. We were therefore prompted to compare the behavior of FeTMPyP with that of an insoluble iron porphyrin adsorbed on EPG electrodes. Iron tetraphenylporphyrin (FeTPP) was selected as representative of the class of insoluble iron porphyrin catalysts that catalyze the reduction of O_2 at potentials considerably positive of the point where the Fe(III) center in the adsorbed porphyrin is reduced to Fe(II) (10).

Electrochemistry of FeTPP Adsorbed on EPG Electrodes. Electrocatalytic Reduction of O_2. In a previous study of adsorbed FeTPP, basal plane graphite electrodes were employed.[10] A feature common to all graphite electrodes is the presence of a somewhat reversible voltammetric response (labeled I in Figure 9B,E) on freshly cleaved or polished electrodes in the absence of any added reactants. This response, which is believed to arise from the reduction and oxidation of functional groups such as quinones that are present on the graphite surface,[9,25-29] can obscure waves associated with adsorbed reactants with reversible potentials that may fall close to potentials where the response from the electrode itself is observed. This is the situation that prevails with FeTPP adsorbed on graphite. Figure 9A is a cyclic voltammogram for a bare EPG electrode and Figure 9B is the response obtained after FeTPP was adsorbed on its surface. The prominent, reversible response at −0.12 V labeled III in Figure 9B,E has been seen in previous studies[10] and corresponds to the $Fe^{III}TPP/Fe^{II}TPP$ couple. There is also a small wave near 0.25 V labeled II in Figure 9B,E that is very close to the background response of the electrode itself (Figure 9A). This wave has not been identified in previous studies. Square wave voltammetry[23,24] is better than cyclic voltammetry for separating closely spaced surface waves so this technique was utilized to inspect the surface waves of FeTPP adsorbed on EPG electrodes (Figure 9D–F). The square wave peaks labeled II and III in Figure 9E correspond to those in the cyclic voltammogram in Figure 9B. They provide clear evidence that adsorption of FeTPP on the EPG electrode produces a redox active adsorbate which exhibits two prominent surface waves that are widely separated in potential.

The new surface wave near 0.25 V could conceivably arise from the free TPP ligand produced by demetalation of FeTPP in the acidic electrolyte employed. This possibility seemed remote be-

(22) Durand, R. R., Jr.; Bencosme, C. S.; Collman, J. P.; Anson, F. C. *J. Am. Chem. Soc.* **1983**, *105*, 2710.
(23) Christie, J. H.; Turner, J. A.; Osteryoung, R. A. *Anal. Chem.* **1977**, *49*, 1899.
(24) Turner, J. A.; Christie, J. H.; Vukovic, M.; Osteryoung, R. A. *Anal. Chem.* **1977**, *49*, 1904.
(25) Garten, V. A.; Weiss, D. E. *Aust. J. Chem.* **1955**, *8*, 68.
(26) Blurton, K. F. *Electrochim. Acta* **1973**, *18*, 869.
(27) Epstein, B. D.; Dalle-Molle, E.; Mattson, J. S. *Carbon* **1971**, *9*, 609.
(28) Randin, J. R.; Yeager, E. *J. Electroanal. Chem. Interfacial Electrochem.* **1975**, *58*, 313.
(29) Evans, J. F.; Kuwana, T. *Anal. Chem.* **1977**, *49*, 1632.

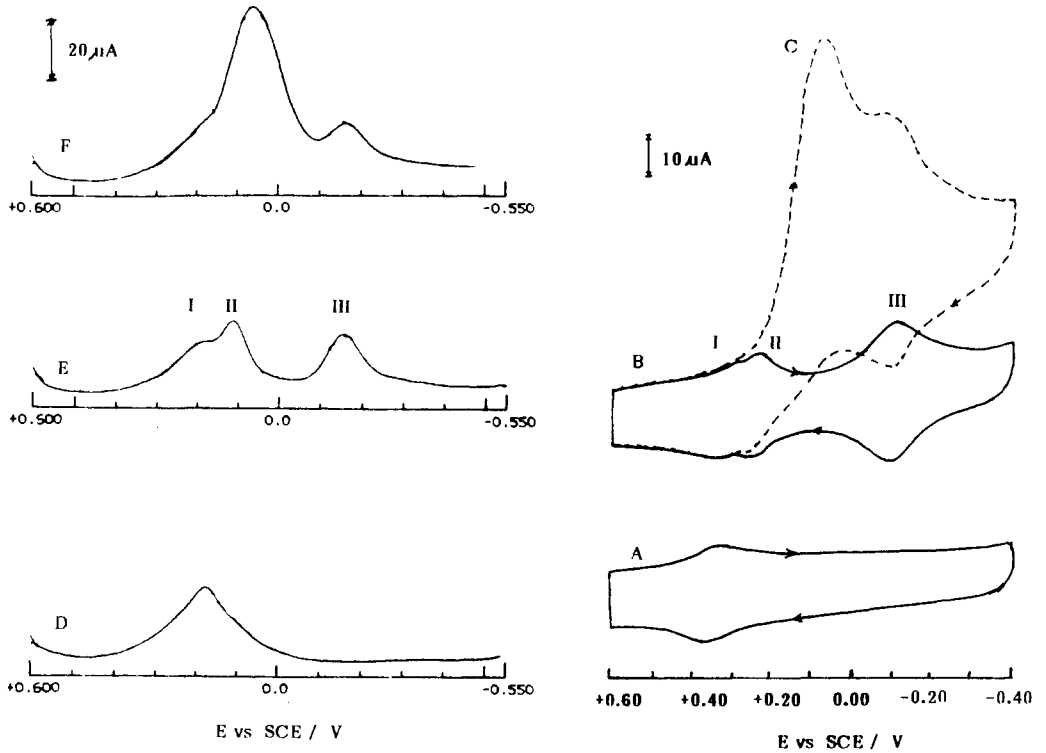

Figure 9. Cyclic and square wave voltammetry of FeTPP adsorbed on an EPG electrode: (A, D) background response for the uncoated EPG electrode; (B, E) after 4.7×10^{-10} mol cm^{-2} of FeTPP was adsorbed on the electrode; (A, B, C) cyclic voltammetry; (D, E, F) square wave voltammetry; (C, F) after the solution was saturated with air. Supporting electrolyte was 0.1 M H_2SO_4. Cyclic voltammetric scan rate was 50 mV s^{-1}. Square wave parameters were the same as those given in Figure 7.

cause the free ligand is not a catalyst for the reduction of O_2. Nevertheless square wave voltammograms were recorded with electrodes on which the metal-free TPP ligand had been adsorbed. The adsorbed ligand exhibited several peaks including one near 0.25 V. However, since none of the other peaks characteristic of adsorbed TPP are present when FeTPP is adsorbed,the peak at 0.25 V in Figure 9B cannot be attributed to the presence of adsorbed TPP.

When O_2 is present in the supporting electrolyte, its catalyzed reduction produces prominent peaks in both cyclic and square wave voltammetry at potentials close to the more positive peak of the adsorbed FeTPP and there is almost no change in the more negative FeTPP peak (Figure 9C,F). It is evident that only the adsorbed FeTPP responsible for the peak near 0.25 V participates in the catalyzed reduction of O_2. Thus, the insoluble FeTPP and the soluble FeTMPyP catalysts share a common feature: adsorption of each on EPG electrodes produces a species with a voltammetric response that appears at potentials significantly more positive than those where the most prominent responses of the original porphyrin appear but close to the potentials where the catalyzed reduction of O_2 occurs.

pH Dependences. Comparisons of the pH dependences of the formal potentials of catalysts adsorbed on the surface of EPG electrodes with the pH dependences of the potentials where the electrocatalyzed reductions of O_2 proceed can be useful in identifying possible catalytic mechanisms and in ruling out others. In Figure 10 the pH dependences of the potentials for a number of electrode processes are summarized. Line A shows the dependence of the "formal potential" of the graphite surface wave obtained with EPG electrodes in reactant-free solutions. The potentials plotted are the averages of the anodic and cathodic peak potentials recorded at 50 mV s^{-1}. The linear plot with a slope near 59 mV per pH unit (the actual slope is 54 mV/pH unit) indicates that one proton per electron is consumed during the reduction of the quinonelike functional groups believed to be generated on the electrode surface during the polishing process.[9,25-29]

The horizontal, cross-hatched region in Figure 10 represents the region where the reduction of O_2 is observed on polished EPG electrodes in the absence of added electrocatalysts. The peak potentials of the uncatalyzed reduction wave (as well as the

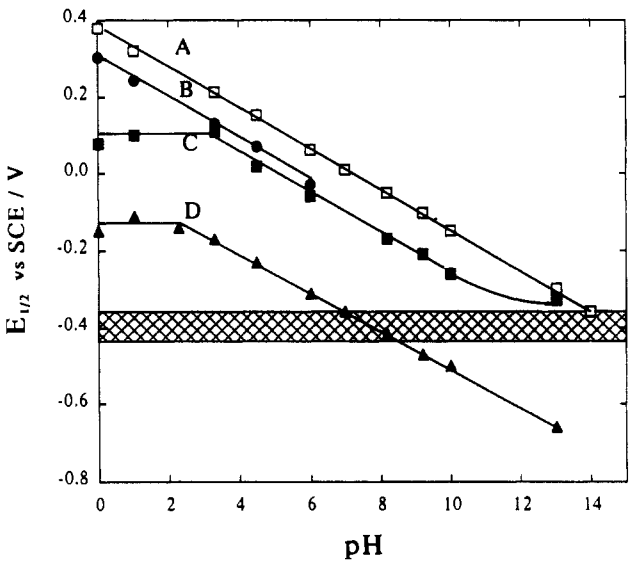

Figure 10. pH dependence of characteristic potentials for adsorbed FeTPP serving as an electrocatalyst for the reduction of O_2 at EPG electrodes: (A) average of cathodic and anodic peak potentials ($E_{p1/2}$) for the surface wave at the freshly polished EPG electrode; (B) $E_{p1/2}$ for peak II in part B of Figure 9; (C) half-wave potential for the reduction of O_2 at a rotating EPG disk electrode coated with 4.7×10^{-10} mol cm^{-2} of FeTPP and rotated at 100 rpm; (D) $E_{p1/2}$ for wave III in Figure 9B. Supporting electrolytes were the buffers listed in the Experimental Section. Scan rates (A, B, D) were 50 mV s^{-1}. The significance of the cross-hatched region is explained in the text.

half-wave potentials at rotating disk electrodes) show essentially no pH dependence but are somewhat sensitive to the polishing procedure and the nature of the buffers employed to adjust the pH. The reproducibility of the measurements is indicated by the height of the cross-hatched region.

The large separation between line A and the cross-hatched region (except at the highest pH values) shows that the electroactive functional groups present on the surface of the EPG electrode are not useful electrocatalysts for the reduction of O_2.

Table I. Effect of the Quantity of Adsorbed FeTPP on the Potential Where O_2 Is Reduced at EPG Electrodes[a]

Γ, mol cm^{-2}	$E_{1/2}$,[d] V vs SCE
$>10^{-9}$	0.13
5×10^{-10} [b]	0.13
1×10^{-10} [b]	0.085
4.7×10^{-11} [c]	0.02
4.7×10^{-12} [c]	0.00

[a] Supporting electrolyte: 0.1 M H_2SO_4 saturated with air. [b] Estimated from the area under the cathodic portion of a cyclic voltammogram recorded at 50 mV s^{-1}. [c] The quantity of FeTPP present in a measured aliquot of a solution in CH_2Cl_2 transferred to the electrode surface with a micropipet. [d] Half-wave potential for O_2 reduction at the coated disk electrode rotated at 100 rpm.

This is not surprising in view of the more negative formal potentials exhibited by the quinone/hydroquinone couples that do act as catalysts for the reduction of O_2 to H_2O_2.[30]

Lines B and D in Figure 10 correspond to the formal potentials of the two waves exhibited by FeTPP adsorbed on the EPG electrode (peaks II and III in Figure 9B,E). Peak II becomes indistinct above pH 6 so that no potentials are plotted for this wave above this pH. However, the catalyzed reduction of O_2 continues to proceed at potentials close to the extrapolation of line B above pH 6 (line C) so that the species responsible for the peaks at lower pH is evidently still present on the electrode surface at pH values where its surface wave becomes indistinct.

The slopes of line B and D are close to 59 mV/pH unit over most of the pH range and this dependence has been attributed in previous studies to the pH dependence of reaction 1, which

$$HOFe^{III}TPP + H^+ + e^- \rightleftarrows H_2OFe^{II}TPP \qquad (1)$$

becomes independent of pH below pH 2 where both oxidation states of the FeTPP are fully protonated (*10*). The continued pH dependence down to pH 0 for line B calls for an alternative explanation that will be addressed in the Discussion section.

Line C in Figure 10 gives the half-wave potentials for the reduction of O_2 at a rotating EPG disk electrode on which FeTPP is adsorbed. The proximity of these $E_{1/2}$ values to those for line B (between pH 4 and 6) and their identical pH dependence (between pH 3 and 6 and probably beyond) strongly suggest that the surface species responsible for line B is the active electrocatalyst for the reduction of O_2. At pH 3 and below, line C becomes horizontal as the half-wave potential of the oxygen reduction wave remains at 0.1 V. This steady potential can be assigned as the (evidently pH independent) value required for the electroreduction of the adsorbed TPP Fe^{II}-O_2 adduct involved in the electrocatalytic mechanism. The pH dependence of line C at pH values above 3 is then understandable as arising from the pH dependence of the reduction potential of the adsorbed Fe^{III}TPP depicted in line B.

The lack of involvement in the catalytic reduction of O_2 of the prominent surface wave for adsorbed FeTPP (wave III in Figure 9B,E) is evident from the position of line D in Figure 10: At all pH values the catalysis occurs at potentials far removed from those where the Fe(III) center in the form of adsorbed FeTPP corresponding to line D is reduced. At pH 13 this difference in potentials becomes even greater as the reduction of O_2 at the EPG surface itself occurs at more positive potentials than those where the adsorbed Fe^{III}TPP is reduced to Fe^{II}TPP.

Effects of Changes in the Quantity of FeTPP Adsorbed. The potential where the catalyzed reduction of O_2 proceeds depends on the quantity of FeTPP adsorbed on the EPG electrode surface as shown in Table I. It was not possible by coulometric assays to obtain reliable estimates for the quantities of the catalytically important form of adsorbed FeTPP because of the overlap of the surface waves for this form of the catalyst and that for the EPG electode itself (Figure 9A,D) so that only values for the quantity of adsorbed inactive catalyst are given in Table I. The active form of the catalyst is apparently present in smaller quantities (Figure 9E). The values of $E_{1/2}$ in Table I become independent of Γ_{FeTPP} at values that correspond to a few monolayers of the inactive form of the catalyst.

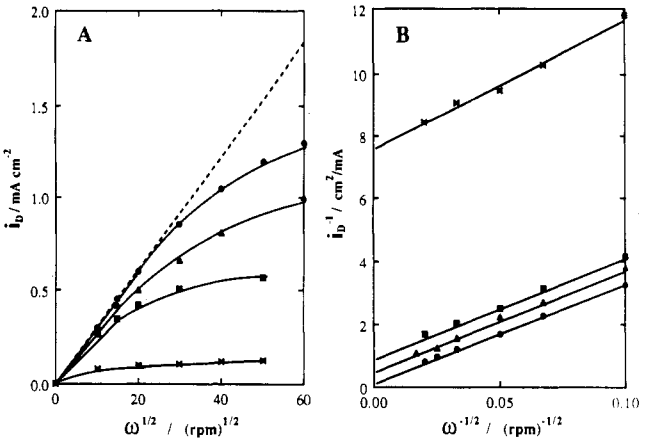

Figure 11. Levich (A) and Koutecky–Levich (B) plots for the reduction of O_2 at EPG electrodes coated with various quantities of FeTPP. Quantities of FeTPP adsorbed on the electrode were (from top to bottom) 5×10^{-10}, 1×10^{-10}, 4.7×10^{-11}, and 4.7×10^{-12} mol cm^{-2}. Supporting electrolyte was 0.1 M H_2SO_4 saturated with air. Solid lines were drawn though the data points. The dashed lines correspond to the four-electron convection-diffusion-limited reduction of O_2.

The plateau currents for the reduction of O_2 at rotating disk electrodes decrease with the quantity of adsorbed catalyst as shown by the Levich plots[19] in Figure 11A. The intercepts of the corresponding Koutecky–Levich plots[20] in Figure 11B were used to estimate the rate of the chemical step that evidently precedes the electroreduction step. This chemical reaction has been[10,31,32] attributed to the formation of an adduct between the adsorbed catalyst and O_2 molecules. As would be expected, the rates obtained from the intercepts of Figure 11B are not proportional to the quantities of inactive catalyst on the surface so that it was not possible to estimate a rate constant for the adduct formation reaction. However, the linearity of the plots in Figure 11B is consistent with the presence of a catalyst on the electrode surface and the species responsible for peak III in Figure 9B,E is clearly *not* the catalyst. Thus, the results are consistent with our identification of the less prominent surface wave for adsorbed FeTPP (wave II in Figure 9B,E) as the catalytically active species in the electroreduction of O_2.

Discussion

Catalyst Adsorption. The results reported in this study make it clear that the effectiveness of complexes capable of catalyzing the reduction of O_2 can be modified significantly by their adsorption on electrode surfaces. Both the water-soluble FeTMPyP catalyst and the insoluble FeTPP catalyst are converted by interactions with the electrode surface into species that operate at more positive potentials. The nature of the interactions with a polished edge plane pyrolytic graphite electrode (EPG) that results in the shift of the reduction potential to more favorable values is, therefore, of considerable interest. The observation that FeTMPyP is not adsorbed in detectable amounts on glassy carbon electrodes but is extensively adsorbed on EPG electrode surfaces suggests that functional groups introduced on the exposed graphite planes during the polishing of the electrode might act as anchors for the adsorbing complexes. However, if the only mode of attachment involved axial coordination to the iron center of the complex by ligands on the graphite surface, one would expect a strong dependence of the extent of adsorption on the oxidation state of the iron. No such dependence is observed, so the adsorption is probably driven by delocalized interactions between

(30) Calabrese, G. S.; Buchanan, R. M.; Wrighton, M. S. *J. Am. Chem. Soc.* **1983**, *105*, 5594.
(31) Collman, J. P.; Marrocco, M.; Denisevich, P.; Koval, C.; Anson, F. C. *J. Electroanal. Chem. Interfacial Electrochem.* **1979**, *101*, 117.
(32) Collman, J. P.; Denisevich, P.; Konai, Y.; Marrocco, M.; Koval, C.; Anson, F. C. *J. Am. Chem. Soc.* **1980**, *102*, 6027.

the porphyrin ring and the electrode surface, possibly including intercalation between the exposed planes of the EPG. However, a substantial specific interaction between the iron center in the adsorbed complex and the electrode surface is required to explain the large shift in the formal potential of the Fe(III)/Fe(II) couple upon adsorption (Figure 2). This shift is toward more positive values so that the Fe(II) form of the complex is more strongly bound by the surface. The coordination chemistry responsible for the positive shift in formal potential could involve back bonding by Fe(II) to unsaturated surface ligands, e.g., carbonyl-like groups, introduced by the polishing of the electrode in air. Thus, one picture of the surface chemistry that accommodates the results involves a graphite surface with a high natural affinity for the porphyrin ring which results in the spontaneous adsorption of FeTMPyP from solution. The presence of unsaturated ligands on the polished EPG surface results in additional, specific interactions with the iron center that produce the difference between the formal potential of the Fe^{III}/Fe^{II} couple in solution and adsorbed on the surface.

The presence of two forms of adsorbed FeTPP on the surface of EPG electrodes (Figure 9) can be understood on the basis of the same picture: The hydrophobic character of the insoluble complex emphasizes its affinity for the graphite surface. Adsorption at sites where unsaturated potential axial ligands are absent results in the voltammetric response at the more negative potentials (Figure 10, line D). The FeTPP that is adsorbed at sites where axial ligands are present participates in the back-bonding interactions that cause the voltammetric response to shift to more positive potentials (Figure 10, line B). That only one form of adsorbed complex is obtained with the soluble FeTMPyP complex might reflect the intrinsically weaker attraction of graphite for this less hydrophobic complex so that a combination of axial coordination and graphite surface–porphyrin ring interaction is required to obtain significant adsorption.

The same interactions with the graphite surface that produce the difference in formal potentials between line B and D in Figure 10 may also be responsible for the pH dependence shown for line B below pH 3. This dependence could reflect a higher acidity of the water molecule coordinated to the Fe(III) center in the form of the adsorbed FeTPP that is reduced at the more positive potentials so that reaction 1 continues to describe the electrode process even at pH 0. Alternatively, it is possible that a weakly basic ligand on the graphite surface which coordinates to the Fe(III), but not the Fe(II), center is protonated upon reduction of the iron center at pH values below 3. In this case, the observed pH dependence would arise from reaction 1 at pH values above 3 and from the protonation of the surface-bound ligand at lower pH values. Whatever its origin, the continued pH dependence of the formal potential of the adsorbed catalyst at low pH values was fortuitous because the divergence of lines B and C in Figure 10 allowed the reduction potential of the $Fe^{II}TPP–O_2$ adduct to be located.

Mechanism of the Catalytic Reduction of O_2. The fact that the adsorption on EPG electrodes of both FeTMPyP and FeTPP produces catalysts that operate at more positive potentials than those corresponding to the dissolved (TMPyP) or the preponderant from (TPP) of these iron porphyrins is intriguing. It suggests that one might be able to obtain catalysts that operate at even more positive potentials if more strongly back-bonding groups could be introduced on the electrode surface. However, there is a limit to the positive shift in the catalyst operating potentials that can be anticipated. The mechanism by which the adsorbed FeTMPyP and FeTPP are believed to operate to catalyze the reduction of O_2 is summarized in eqs 2–4, where $Fe^{III}P$ and $Fe^{II}P$ represent

$$Fe^{III}P + e \overset{E_1}{\rightleftharpoons} Fe^{II}P \quad (2)$$

$$Fe^{II}P + O_2 \underset{k_b}{\overset{k_f}{\rightleftharpoons}} Fe^{II}P–O_2 \quad (3)$$

$$Fe^{II}P–O_2 + ne \xrightarrow{E_2} Fe^{II}P + H_2O, H_2O_2 \quad (4)$$

the oxidized and reduced forms of the adsorbed porphyrins, respectively, and E_1 is the formal potential of the adsorbed, electrocatalytically active Fe^{III}/Fe^{II} porphyrin couple. E_1 is pH dependent over much of the range between 0 and 14 (Figure 10) because of reaction 1. The equilibrium in reaction 3 lies well to the left in aqueous media and the plateau currents at catalyst-coated rotating disk electrodes can be limited by the forward rate of reaction 3.[10] Evidence that the equilibrium binding of O_2 to the reduced catalyst is not extensive can be found in the square-wave voltammetric peak corresponding to the catalytically active form of the adsorbed FeTPP in Figure 9E. The peak remains at essentially the same potential in the presence of O_2 (Figure 9F). A shift of this peak potential to more positive potentials would be expected if a significant fraction of the reduced porphyrin were converted to the O_2 adduct. The lack of a shift in peak potential in air-saturated solutions allows an upper limit of ca. 4×10^2 M^{-1} to be placed on the equilibrium constant for reaction 3 in the case of FeTPP.

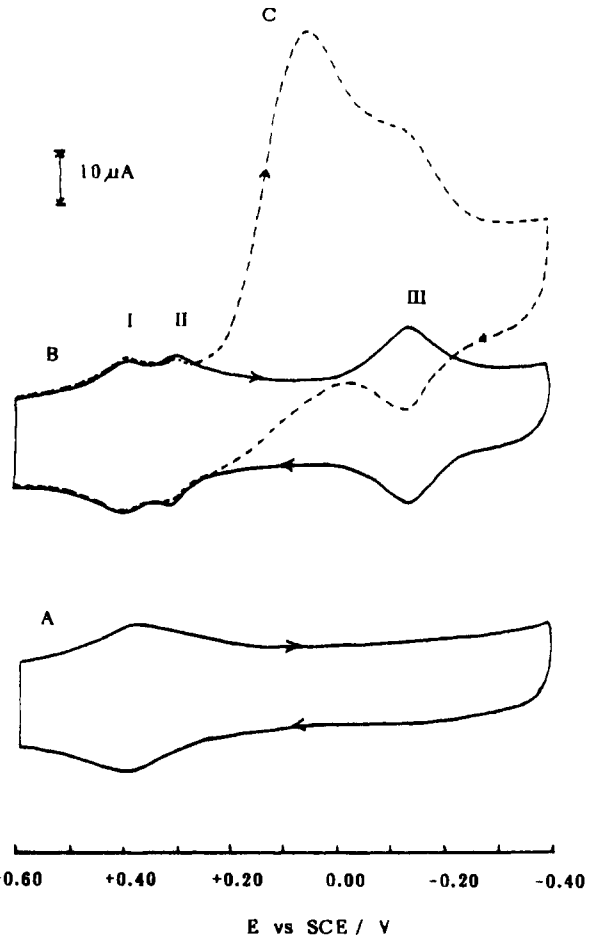

Figure 12. Cyclic voltammetry of adsorbed FeTPP and O_2 reduction at pH 0: (A) background response for the uncoated EPG electrode; (B) after 4.7×10^{-10} mol cm^{-2} of FeTPP was adsorbed on the electrode; (C) after the solution was saturated with air. Supporting electrolyte was 1.0 M H_2SO_4. Scan rate was 50 mV s^{-1}.

The irreversible reduction of the adduct formed in reaction 3 occurs at potential E_2. This potential is evidently independent of pH in the case of FeTPP (Figure 10). It is apparent from the mechanism shown in reactions 2–4 that it would be unproductive to shift E_1 to values more positive than E_2. For FeTPP, E_2 is about 0.1 V (Figure 10). When the formal potential of the adsorbed catalyst is shifted to potentials more positive than 0.1 V by decreasing the pH below 3 (Figure 10 line B), the potential where the catalyzed reduction of O_2 proceeds (Figure 10, line C) no longer follows the formal potential of the Fe(III)/Fe(II) couple and a catalyst surface wave appears ahead of the O_2 reduction wave at low pH (Figures 9F and 12). The first wave after the response from the EPG surface itself corresponds to the reduction of the adsorbed $Fe^{III}TPP$ to $Fe^{II}TPP$, which can form an adduct with O_2. However, the adduct cannot be reduced at the potentials

where the $Fe^{II}TPP$ is formed so that no catalytic reduction ensues until the potential approaches 0.1 V where the $Fe^{II}TPP–O_2$ adduct *is* reducible. (The final wave in Figure 12C arises from the reduction of the second form of adsorbed FeTPP that does not participate in the catalysis.)

The behavior shown in Figures 9F, 10, and 12 demonstrates the lack of reduction of O_2 by the $Fe^{II}TPP$ which is generated at potentials positive of 0.1V. This behavior provides strong evidence against an alternative reaction mechanism in which the first step following the electroreduction of the catalyst is simple, outer-sphere electron transfer between $Fe^{II}TPP$ and O_2. Such a mechanism has been proposed for the catalysis of O_2 reduction by iron porphyrins in solution,[9] but it can be ruled out for adsorbed FeTPP on the basis of the reaction pattern shown in Figures 9F, 10, and 12. The behavior of the adsorbed FeTPP and FeTMPyP catalysts, in which reduction of the adsorbed catalyst occurs at potentials ahead of those where the catalyzed reduction of O_2 proceeds, is the same as that exhibited by the corresponding cobalt porphyrin, CoTPP, where the reduction of $Co^{III}TPP$ to $Co^{II}TPP$ occurs at potentials much more positive than those where CoTPP serves as a catalyst for the reduction of O_2.[33] Thus, the behavior of iron and cobalt porphyrins in catalyzing the electroreduction of O_2 can be rationalized by means of a single reactivity pattern: The catalytic reduction of O_2 can occur at potentials no more positive than that at which the metal center in the metalloporphyrin is reduced from the +3 oxidation state, which does not interact with O_2, to the +2 oxidation state, which does. For cobalt porphyrins, this potential is much more positive than that where the electroreduction of O_2 is observed. The latter potential corresponds to the intrinsic reduction potential of the cobalt porphyrin–dioxygen adduct, which is evidently significantly more negative than the formal potential of the Co^{III}/Co^{II} couple of the cobalt porphyrin. In the case of iron porphyrins, E_2 (reaction 4) is more positive than E_1 (reaction 2) (except at low pH values). The result is a close correspondence between the potential where the iron(III) center in the catalytically relevant adsorbed porphyrin is reduced in the absence of O_2 and that where the catalyzed reduction of O_2 appears. The apparent mismatch between these two potentials that was emphasized in previous studies[10] of several iron porphyrins has been shown in the present work to disappear when adequate account is taken of the effect of adsorption on graphite on the formal potentials of the iron porphyrins.

Acknowledgment. This work was supported by the National Science Foundation.

(33) Ni, C.-L.; Anson, F. C. *Inorg. Chem.* **1985**, *24*, 4754.

Contribution from the Department of Chemistry and Biochemistry, San Francisco State University, San Francisco, California 94132

Chemical and Electrochemical Reduction of Binuclear Platinum Phosphine Complexes

Jane V. Zeile Krevor* and Lawrence Yee

Received January 31, 1990

Two synthetic methods are described to produce platinum(0) complexes that contain two metal atoms held together by bridging phosphine ligands. Both platinum(I) and platinum(II) complexes are reduced by using chemical and electrochemical techniques to produce the desired platinum dimers. The electrochemistry and the solution chemistry of these complexes are investigated by cyclic voltammetry and NMR experiments. The formation of platinum hydride complexes is shown to be an important step in the electrochemical reactions.

Introduction

Platinum has played a major role in the catalytic rearrangement of hydrocarbons.[1] For that reason the study of platinum complexes has been and continues to be important. In particular, the platinum complexes that contain hydrocarbon units have been investigated as possible homogeneous complexes that may mimic intermediates proposed to be present on a platinum surface during catalysis.[2] Recently, both platinum(0) phosphine complexes[3] and platinum phosphine dimers[4] have received much attention because of their interesting reaction chemistry and their own potential as catalysts.

We became particularly intrigued with the report of a Pt(0) dimer, $Pt_2(dppm)_3$, where dppm = bis(diphenylphosphino)-methane,[5,6] which readily participated in oxidative addition reactions with iodoalkanes, yet was stable enough to be characterized by crystallographic methods.[7] Keeping two platinum(0) atoms adjacent to one another with bridging phosphine ligands makes this dimer more analogous to metallic sites on a platinum surface than previously reported platinum dimers. So far, only one other platinum(0) dimer has been isolated.[8] Therefore, we sought to

(1) (a) Satterfield, C. N. *Heterogeneous Catalysis in Practice*; McGraw-Hill: New York, 1980; p 247. (b) Gates, B. C.; Katzer, J. R.; Schuit, G. C. A. *Chemistry of Catalytic Processes*; McGraw-Hill: New York, 1979; p 267. (c) Masters, C.; *Homogeneous Transition-Metal Catalysis—a gentle art*; Chapman and Hall: London, 1981; p 132. (d) Parshall, G. W. *Homogeneous Catalysis*; J. Wiley & Sons: New York, 1980; p 72.

(2) (a) Shilov, A. E.; Steinman, A. A. *Coord. Chem. Rev.* **1977**, *24*, 97. (b) Foley, P.; DiCosimo, R.; Whitesides, G. M. *J. Am. Chem. Soc.* **1980**, *102*, 6713. (c) DiCosimo, R.; Moore, S. S.; Sowinski, A. F.; Whitesides, G. M. *J. Am. Chem. Soc.* **1982**, *104*, 124. (d) Stone, F. G. A. *Acc. Chem. Res.* **1981**, *14*, 318. (e) Brown, D. B.; Viens, V. A. *J. Organomet. Chem.* **1977**, *142*, 117.

(3) (a) Bennett, M. A.; Yoshida, T. *J. Am. Chem. Soc.* **1978**, *100*, 1750. (b) Cook, C. D.; Jauhal, G. S. *J. Am. Chem. Soc.* **1968**, *90*, 1464. (c) Davies, J. A.; Eagle, C. T.; Otis, D. E.; Venkataraman, U. *Organometallics* **1986**, *5*, 1264. (d) Scott, J. D.; Puddephatt, R. J. *Organometallics* **1986**, *5*, 1253. (e) Caspar, J. V. *J. Am. Chem. Soc.* **1985**, *107*, 6718.

(4) (a) Brown, M. P.; Puddephatt, R. J.; Rashidi, M.; Seddon, K. R. *J. Chem. Soc., Dalton Trans.* **1976**, 951. (b) Chin, C. S.; Sennett, M. S.; Wear, P. J.; Vaska, L. *Inorg. Chim. Acta* **1978**, *31*, 443. (c) Minghetti, G.; Bandini, A. L.; Banditelli, G.; Bonati, F.; Szostak, R.; Strouse, C. E.; Knobler, C. B.; Kaesz, H. D. *Inorg. Chem.* **1983**, *22*, 2332. (d) Muralidharan, S.; Espenson, J. H.; Ross, S. A. *Inorg. Chem.* **1986**, *25*, 2557. (e) Afzal, D.; Lukehart, C. M. *Organometallics* **1987**, *6*, 546.

(5) Grossel, M. C.; Brown, M. P.; Nelson, C. D.; Yavari, A.; Kallas, E.; Moulding, R. P.; Seddon, K. R. *J. Organomet. Chem.* **1982**, *232*, C13.

(6) Brown, M. P.; Yavari, A.; Hill, R. H.; Puddephatt, R. J. *J. Chem. Soc., Dalton Trans.* **1985**, 2421.

(7) Manojlovic-Muir, L.; Muir, K. W. *J. Chem. Soc., Chem. Commun.* **1982**, 1155.

(8) Yoshida, T.; Yamagatya, T.; Tulip, T. H.; Ibers, J. A.; Otsuka, S. *J. Am. Chem. Soc.* **1978**, *100*, 2063.

0020-1669/90/1329-4305$02.50/0